Delithiation of $LiFePO_4$ with Cl_2 Gas: Preparation of $FePO_4$ for Sodium-Ion Batteries with High Li Recovery

Fumiyasu Nozaki, Sho Shomura, Jinkwang Hwang, Kazuhiko Matsumoto,* Rika Hagiwara*

Graduate School of Energy Science, Kyoto University, Yoshida-honmachi, Sakyo-ku, Kyoto 606-8501, Japan

*Corresponding Authors

E-mail: k-matsumoto@energy.kyoto-u.ac.jp (K. M.) and hwang.jinkwang.5c@kyoto-u.ac.jp (J. H.)

ABSTRACT

Triphylite $NaFePO_4$ is considered a promising positive electrode for sodium-ion batteries due to its exclusive composition of abundant elements, high thermal stability, and theoretical capacity (154 mAh g^{-1}). However, the low thermodynamic stability of triphylite $NaFePO_4$ precludes direct synthesis techniques such as the solid-state route, thus hampering its commercial viability. Herein, we report a novel preparation of heterosite $FePO_4$, a triphylite $NaFePO_4$ desodiation product, through the delithiation of triphylite (olivine) $LiFePO_4$ using Cl_2 gas. Besides the scalability prospects, the present technique efficiently recovers the lithium source in a utilitarian form. The prepared $FePO_4$ electrode yields a high reversible capacity of 127 mAh $(g\text{-}FePO_4)^{-1}$ at 0.05C (1C = 154 mA g^{-1}) and good cycling performance (capacity retention of 98.5% after 250 cycles at 1C). X-ray diffraction (XRD) revealed the reversible phase transition between heterosite $FePO_4$ and triphylite $NaFePO_4$ during charge-discharge.

Keywords

$LiFePO_4$, $NaFePO_4$, heterosite $FePO_4$, olivine, triphylite, sodium ion-batteries

INTRODUCTION

As the world steers toward environmentally benign materials, sodium-ion batteries (SIBs) have emerged as promising alternatives to lithium-ion batteries (LIBs) owing to the abundance and extensive distribution of sodium resources.[1, 2] Besides sustainability, sodium manifests chemical properties similar to lithium because of their proximity in the periodic table (Group 1 elements), betokening the possibility of battery systems comparable to LIBs.[3-5] Even so, SIB advancement is heavily encumbered by insufficient capacities due to the scarcity of positive electrode materials, especially the elements (such as transition metals) for their redox centers. Thus, the possibility of high-performance positive electrodes employing abundant elements would be a significant milestone for high-energy-density SIB.

The search for SIBs positive electrodes has galvanized explorations into polyanionic materials, such as phosphates and pyrophosphates ($Na_3V_2(PO_4)_3$, $Na_3V_2(PO_4)_2F_3$, $Na_2FeP_2O_7$, etc.) in attempts to emulate the electrochemical performances of their Li analogs in LIBs.[6-11] In particular, $NaFePO_4$ positive electrodes have demonstrated remarkable structural stability, high energy density, and stable electrochemical behavior.[12-14] The olivine $NaFePO_4$ is known to crystalize in two polymorphs, maricite and triphylite (so-called olivine structures in Li-based systems). The maricite $NaFePO_4$ has high thermodynamic stability that allows solid-state or hydrothermal syntheses at high temperature. However, this polymorph has limited Na^+ diffusion paths and a high diffusion barrier which generally results in low electrochemical performance.[14-20] In search of solutions, a study reported that the desodiation of a nano-sized maricite $NaFePO_4$ formed an amorphous $FePO_4$ with significantly enhanced Na^+ mobility.[21] Other studies have also shown that reducing the particle sizes and elevating cell operation temperature to 90 °C partially activated the maricite $NaFePO_4$ and improved charge-discharge capacity.[17, 22]

Against this backdrop, triphylite $NaFePO_4$ has been reported to embody Na^+ diffusion paths along the [101] direction, much like triphylite $LiFePO_4$, which renders positive electrodes with substantial performances (capacity of ~120 mAh g^{-1}).[14-16, 23] Despite these prospects, the direct synthesis of triphylite $NaFePO_4$ remains a challenge because the thermodynamically unstable triphylite phase easily converts to the maricite phase when heated above 480 °C.[15, 24] Therefore, triphylite $NaFePO_4$ is typically prepared through chemical or electrochemical delithiation from triphylite $LiFePO_4$ (See Table S1 for the summary of delithiation and sodiation methods, Supporting Information).[15, 23, 25-29] Delithiation engenders a structure known as heterosite $FePO_4$ whose framework is identical to that of triphylite $LiFePO_4$ without the Li atoms. It should be mentioned that although electrochemical delithiation is a common synthesis method in studies entailing triphylite $NaFePO_4$, the process has limited commercial feasibility.[23, 25, 30] Similarly, the practicality of the chemical delithiation process, which uses oxidizing reagents such as nitronium tetrafluoroborate ($[NO_2][BF_4]$) in acetonitrile,[15, 26-28] is heavily limited by the cost and difficulty in handling $[NO_2][BF_4]$. In an attempt to alleviate these handicaps, Berlanga et al. recently proposed a low-cost and eco-friendly synthesis method wherein $Na_2S_2O_8$ was used for delithiation and $Na_2S_2O_3$ for sodiation to produce the triphylite $NaFePO_4$ and sufficiently recover the lithium sources.[29] There is another delithiation method of $LiFePO_4$ using peracetic acid, and the resulting $FePO_4$ showed better rate performance than the one delithiated by $[NO_2][BF_4]$.[30] Other delithiation methods using $K_2S_2O_8$ solution under microwave condition[31] and formic acid with H_2O_2[32] have been also reported as a green method. Compared to these methods, Cl_2 gas treatment is also a pro-environmental method because Cl_2 gas has sufficient reactivity to complete the reaction and the extracted lithium source is efficiently recovered. Furthermore, the residual Cl_2 gas can be easily recovered and reused even if excess Cl_2 was employed.

It is worth noting that the desodiation (or delithiation) of polyanion frameworks is not limited to chemical or electrochemical processes. In fact, a previous report demonstrated that Cl_2 gas treatment of $Na_3V_2(PO_4)_3$ could effectively produce desodiated $NaV_2(PO_4)_3$ (or the two-phase mixture of $Na_3V_2(PO_4)_3$ and $NaV_2(PO_4)_3$, depending on the reaction conditions) which was used to devise a reference electrode for a two-electrode SIB configuration.[33] Compared to the conventional delithiation (or desodiation) techniques, the use of an oxidative gas shortens the reaction durations and improves the scalability of the process. The use of a nonaqueous medium (acetonitrile here) also has a high applicability to various materials because many positive electrode materials are unstable in aqueous media, especially in the charged state.

In an effort to augment the viability of $NaFePO_4$ positive electrodes for SIBs, this paper presents a novel preparation method for heterosite $FePO_4$. Here, a triphylite (olivine) $LiFePO_4$ is delithiated using Cl_2 gas to produce the heterosite $FePO_4$ and recover Li in the form of $LiAlCl_4$ (Figure 1). The obtained heterosite $FePO_4$ is characterized through X-ray diffraction (XRD) and the Rietveld refinement to ascertain its crystal structure. Scanning electron microscopy (SEM) and energy dispersive X-ray (EDX) spectrometry are employed to confirm the morphology and elemental composition before and after the delithiation process. The electrochemical properties of the positive electrode are further evaluated through a series of electrochemical performance tests.

EXPERIMENTAL SECTION

Materials and Handling. All moisture- and oxygen-sensitive materials were handled under a dry Ar atmosphere (H_2O < 1 ppm and O_2 < 1 ppm) in a glove box. The materials sensitive to the moisture in air were handled under a dry air atmosphere in an open dry chamber. The reagents: $LiFePO_4$/C (Toshima Manufacturing, purity 99.9%, carbon coating: 1.15%), acetonitrile (Fujifilm

Wako Pure Chemicals, super dehydrated, H_2O < 10 ppm, purity > 99.8%), $AlCl_3$ (Fujifilm Wako Pure Chemicals, purity 98.0%), and Cl_2 gas (Sumitomo Seika Chemicals, purity > 99.4%), were used as-purchased for the delithiation process. Sodium metal (Sigma-Aldrich, purity 99.95%), Super C65 (MTI Corp.), 1 mol dm^{-3} Na[PF_6]-EC/DMC (1:1 v/v) (Kishida Chemical, battery grade), fluoroethylene carbonate (FEC, Fujifilm Wako Pure Chemicals), polyvinylidene fluoride (PVDF, Kureha Corp.), and *N*-methylpyrrolidone (NMP, Fujifilm Wako Pure Chemicals, purity > 99.0%) were used for cell assembly.

Delithiation of $LiFePO_4$. Under a dry air atmosphere, 7.8885 g (50.003 mmol) of $LiFePO_4$/C, 8.0156 g (60.114 mmol) of $AlCl_3$, and approximately 50 mL of acetonitrile were added into an air-tight glass reaction vessel. The vessel was evacuated before slowly introducing 100 kPa of Cl_2 gas (26.5 mmol) from a storage cylinder via a reaction manifold.[33] The mixture was left undisturbed in the reaction vessel for 72 h. After the reaction, all the volatile gases were evacuated through a liquid nitrogen cold trap. The reaction product was washed with acetonitrile several times to remove $LiAlCl_4$ and dried at 60 °C under a vacuum for two days to obtain $FePO_4$/C powder.

Characterizations. X-ray diffraction (XRD) patterns of the samples were collected using a Rigaku SmartLab diffractometer (Ni filtered Cu-*K*α, 40 kV-30 mA, scan rate: 0.1° min^{-1}). The Rietveld refinement of the obtained XRD patterns was performed using the FullProf software.[34] The samples were subjected to scanning electron microscopy (SEM, SU-8020, Hitachi) for surface observation. The element composition of the samples was obtained by energy dispersive X-ray spectroscopy analysis (EDX, EMAXEvolution X-max, Horiba).

Preparation of Electrode. The electrode was prepared by mixing the obtained $FePO_4$/C with Super C65 carbon and PVDF (80:15:5wt%) in NMP using a planetary mixer (AR-100, Thinky).

The mixture was thereafter pasted onto an Al foil and dried under vacuum for 2 h at room temperature and overnight at 80 °C. The dried electrode was punched into discs (diameter: 10 mm).

Preparation of Coin Cells. Type-2032-coin cells were assembled in a glove box under a dry Ar atmosphere. The sodium metal negative electrode was cut into a disk (diameter: 13 mm) and attached to an Al plate current collector. The $FePO_4$/C electrode prepared in the method described above was used as a positive electrode. A 1 mol dm^{-3} Na[PF_6]-EC/DMC (1:1 v/v) with 3wt% of FEC additive was selected as the electrolyte. A glass microfiber (Whatman GF/D) was used as a separator.

Electrochemical Measurements and Characterization of Electrode. Charge-discharge properties, rate capabilities, and cycle performance were evaluated using a charge-discharge test device (HJ1001SD8, Hokuto Denko) at 25 °C. The capacity was calculated based on the weight of the $FePO_4$ active material. The cutoff voltage for the tests was set in the 2.0–3.8 V range. After the charge-discharge tests, the coin cells were disassembled, and the electrodes were characterized by XRD.

RESULTS AND DISCUSSION

In this study, $FePO_4$/C powder was obtained through the delithiation of $LiFePO_4$/C using Cl_2 gas, in accordance with the following reaction (1):

$$2LiFePO_4 + 2AlCl_3 + Cl_2 \rightarrow 2FePO_4 + 2LiAlCl_4 \quad (1)$$

Here, Cl_2 gas works as an oxidizing agent while $AlCl_3$ acts as a Lewis acid for dissolving the LiCl formed on the surface of $LiFePO_4$.[33] Most notably, the Cl_2 gas used in this reaction makes

this preparation process uniquely expedient for mass production while ensuring a high recovery efficiency of the lithium source. This reaction can theoretically recover 100% of lithium in the form of $LiAlCl_4$ using acetonitrile. In the present method, the $LiAlCl_4$ dissolved in acetonitrile was separated from $FePO_4$/C through simple filtration or centrifuge. The lithium recovery ratio is obtained as 97.4% (see Supporting Information in details of calculation). Notably, the recovered $LiAlCl_4$ is expected to gain utility in various applications that augment the economic viability of this method. For example, the $LiAlCl_4$ can be used directly as an electrolyte for lithium/thionyl chloride primary batteries which are known for their high energy densities and long lifetimes.[35, 36] Other works have also suggested that this byproduct can be used as electrolytes in solid-state or in SO_2 solutions for LIBs.[37-39] Furthermore, chemical conversion through hydrolysis or metathesis can also yield other lithium compositions.

X-ray diffraction (XRD) patterns of the obtained $FePO_4$/C (heterosite, space group: *Pnma*) and the pristine $LiFePO_4$/C (triphylite, space group: *Pnma*) are illustrated in Figure 2 for comparison. The patterns were also analyzed through the Rietveld refinement (see Tables S2 and S3 for crystallographic data of $LiFePO_4$/C and $FePO_4$/C, Supporting Information). The XRD pattern of the obtained $FePO_4$/C corresponds with that of $FePO_4$ heterosite, albeit with some impurity peaks assigned to $LiFePO_4$.[40] The weight fractions of $FePO_4$ (98.0%) and $LiFePO_4$ (2.0%) phases, determined through the Rietveld quantitative phase analysis, verified the high efficacy of the preparation method. The small charge capacity in the charge curve of the Na/$FePO_4$ cell shown in Figure S1 (Supporting Information) also indicates that lithium is adequately extracted and the remaining lithium has a very limited impact on the electrochemical performance of the SIB.

The scanning electron microscopy (SEM) images and the energy dispersive X-ray spectroscopy (EDX) mappings of the obtained $FePO_4$/C and the pristine $LiFePO_4$/C are shown in

Figure 3. The SEM images reveal that the present delithiation process did not damage the morphology of the pristine particles. The EDX analysis of the obtained $FePO_4$/C and the pristine $LiFePO_4$/C identifies that the carbon contents of both materials are almost the same, indicating that this Cl_2 gas treatment did not damage the carbon coating of the pristine $LiFePO_4$. The EDX mapping images, obtained at the same magnification level, display an even distribution of all the elements across the obtained $FePO_4$/C particles. Additionally, the EDX results show that only 0.1% of Cl is present on the $FePO_4$/C surface, confirming that the byproduct was adequately removed from the product (see Table S4 for detailed amount of each element, Supporting Information).

The electrochemical performance of the Na/$NaFePO_4$ cell is highlighted in Figure 4. The current densities are expressed as C-rates of $NaFePO_4$ (theoretical capacity of 154 mAh g^{-1}). Prior to the electrochemical performance tests, the $FePO_4$ electrode was discharged at 0.05C for sodiation (see the preliminary discharge curve of the Na/$FePO_4$ cell in Figure S2, Supporting Information). The electrode achieved a discharge capacity of 127 mAh $(g\text{-}FePO_4)^{-1}$, comparable performance with chemically or electrochemically prepared $NaFePO_4$ in previous works.[23, 25, 26, 41] The preliminary discharge curve also exhibited a slightly larger overpotential that was attributed to the reconstruction of the surface layer between electrode and electrolyte. [25] After the preliminary discharge, charge-discharge curves were obtained at 0.05C. Figure 4(a) shows the charge process entails a single-phase reaction ranging from $NaFePO_4$ to $Na_{2/3}FePO_4$, followed by a two-phase reaction ranging from $Na_{2/3}FePO_4$ to $FePO_4$.[15, 25, 42, 43] However, these reaction ranges cannot be clearly discerned from the discharge curves (see the *ex-situ* XRD results below for the assignments of the plateaus). These results are attributed to the kinetics of (de)sodiation process, wherein Na^+ mobility during the phase transformation between $FePO_4$ and $Na_{2/3}FePO_4$ is slower than in the

solid-solution region between $Na_{2/3}FePO_4$ and $NaFePO_4$.[25] Figure 4(b) shows the rate capability at varied C-rates. The measurements performed at 0.1C, 0.2C, 0.5C, 1C, and 2C provided discharge capacities of 100, 88, 71, 60, and 50 mAh $(g\text{-}FePO_4)^{-1}$, respectively. The charge-discharge curves obtained during the rate capability tests (Figure S3, Supporting Information) demonstrate increased polarization at higher current densities, evincing that the poor kinetics during the desodiation/sodiation reactions resulted from the low diffusivity of Na^+ and/or the high phase transformation barrier in Na_xFePO_4. The low diffusivity of Na^+ is ascribed to the rigid $\cdots{-}PO_4{-}Fe{-}PO_4{-}\cdots$ framework, which impedes the movement of the larger-sized Na^+ (compared to Li^+).[41] As shown in Figure 4(c), the cycle performance at 0.2C yielded an initial discharge capacity of 72 mAh $(g\text{-}FePO_4)^{-1}$ and an average coulombic efficiency of 99.9% for 150 cycles. During cycling, the discharge capacity was observed to increase gradually, reaching 88 mAh $(g\text{-}FePO_4)^{-1}$ at the 150th cycle. One possible reason for the increase is the increase in active sites because of the deagglomeration of particles during the cycle. On the other hand, the cycle performance at 1C (Figure 4(d)) achieved an initial discharge capacity of 69 mAh $(g\text{-}FePO_4)^{-1}$ and remarkably maintained an average coulombic efficiency of 98.9% for 1000 cycles. Additionally, the electrode exhibited excellent capacity retentions of 98.5%, 97.1%, and 88.6% after the 250th, 500th, and 1000th cycles, respectively. The corresponding charge-discharge curves in Figures S4 and S5 (Supporting Information) appear to overlap each other throughout the cycles, evidencing the high reversibility of the mechanisms. The excellent cycle performance observed indicates that delithiation using Cl_2 does not damage the host framework of the pristine $LiFePO_4$. In addition, this electrochemical performance indicates Cl_2 gas treatment can preserve the carbon coating of the pristine $LiFePO_4$ and keep good electronic conductivity of the material.

An XRD pattern of the discharged electrode after 1000 cycles (Figure S6(a), Supporting Information) shows the triphylite $NaFePO_4$ structure (space group: *Pnma*)[15] was maintained throughout cycling. The absence of a phase transition to maricite validates the high structural stability of this framework. The SEM image obtained after the electrode was carefully washed demonstrates that the distinct shape of particles was preserved with no sign of cracks or deposits from electrolyte decomposition. Although EDX analysis (Figure S6(b) and Table S5, Supporting Information) can only approximate the elemental composition, the obtained Na/Fe ratio of 1.06 suggests that the sodiation process has high reversibility throughout the 1000 cycles.

The phase transition mechanism during charge-discharge was determined through *ex-situ* XRD analyses of $FePO_4$/C electrodes at different states of charge, as shown in Figure 5. Before the charge-discharge test, the electrode manifests peaks belonging to the heterosite $FePO_4$[23] (Pattern (1), Figure 5). After discharge to 2.0 V, the diffraction pattern shows that a triphylite $NaFePO_4$[15] (Pattern (2), Figure 5) is formed. This suggests that Na-ion insertion into the heterosite $FePO_4$ involves a Fe^{III}/Fe^{II} reaction accompanied by a structural transformation to the triphylite $NaFePO_4$. However, this pattern retains some $FePO_4$ peaks since the discharge capacity obtained is lower than the theoretical capacity. The XRD pattern obtained at the state of charge of 32% during charging confirms the existence of a $Na_{2/3}FePO_4$ intermediate phase (space group: *Pnma*) [15, 25, 42, 43] with diffraction peaks at higher angles than those of $NaFePO_4$ (Pattern (3), Figure 5). This structural change validates the single-phase reactions exhibited by the charge curves in Figure 4(a). After charging the electrode to 3.8 V, majority of the peaks displayed were ascribed to the $FePO_4$ (Pattern (4), Figure 5), demonstrating the high reversibility of the two-phase sodiation/desodiation reaction between heterosite $FePO_4$ and triphylite $Na_{2/3}FePO_4$. Even so, peaks

ascribed to residual $Na_{2/3}FePO_4$ were also noted, signifying incomplete charging due to the low diffusion coefficient of Na^+.[41]

CONCLUSION

Herein, we report a novel preparation for a heterosite $FePO_4$ positive electrode for SIBs through the delithiation of $LiFePO_4$/C using Cl_2 gas. The heterosite framework of the obtained $FePO_4$/C electrode is ascertained through a combination of XRD analyses and the Rietveld refinement. Charge-discharge tests demonstrate a high reversible capacity of 127 mAh $(g\text{-}FePO_4)^{-1}$ at 0.05C, indicating comparable performance with previously reported $NaFePO_4$. Additionally, the electrode exhibits excellent cycling performance at 1C with high capacity retentions of 98.5%, 97.1%, and 88.6% after 250, 500, and 1000 cycles, respectively. *Ex-situ* XRD analyses confirm the sodiation/desodiation mechanisms involve highly reversible phase transitions between the heterosite $FePO_4$ and triphylite $NaFePO_4$ via an intermediate $Na_{2/3}FePO_4$ phase. This study establishes delithiation using Cl_2 gas as an effective technique for the mass production of highly stable triphylite structures.

Supporting Information.

The Supporting Information is available free of charge at DOI: xx. Details on the calculation of lithium recovery ratio; summary of previously reported preparation methods for triphylite $NaFePO_4$ from olivine $LiFePO_4$; crystallographic parameters of $LiFePO_4$ and $FePO_4$; Electrochemical properties, XRD, SEM, and EDX data for the electrode materials (PDF).

AUTHOR INFORMATION

Corresponding Authors

Kazuhiko Matsumoto − Graduate School of Energy Science, Kyoto University, Yoshida-honmachi, Sakyo-ku, Kyoto 606-8501, Japan; orcid.org/0000-0002-0770-9210; E-mail: k-matsumoto@energy.kyoto-u.ac.jp

Jinkwang Hwang − Graduate School of Energy Science, Kyoto University, Yoshida-honmachi, Sakyo-ku, Kyoto 606-8501, Japan; orcid.org/0000-0003-4800-3158; Email: hwang.jinkwang.5c@kyoto-u.ac.jp

Authors

Fumiyasu Nozaki − Graduate School of Energy Science, Kyoto University, Yoshida-honmachi, Sakyo-ku, Kyoto 606-8501, Japan; orcid.org/ 0000-0003-4399-3578

Sho Shomura − Graduate School of Energy Science, Kyoto University, Yoshida-honmachi, Sakyo-ku, Kyoto 606-8501, Japan

Rika Hagiwara − Graduate School of Energy Science, Kyoto University, Yoshida-honmachi, Sakyo-ku, Kyoto 606-8501, Japan; orcid.org/0000-0002-7234-3980

Notes

The authors declare no competing financial interest.

ACKNOWLEDGMENT

This study was supported by JSPS Grant-in-Aid for Scientific Research (B) Grant Number 21H02047 and JST SPRING Grant Number JPMJSP2110.

REFERENCES

(1) Yan, G.; Mariyappan, S.; Rousse, G.; Jacquet, Q.; Deschamps, M.; David, R.; Mirvaux, B.; Freeland, J. W.; Tarascon, J.-M. Higher energy and safer sodium ion batteries via an electrochemically made disordered $Na_3V2(PO_4)_2F_3$ material. *Nat. Commun.* **2019**, *10*, 585, DOI 10.1038/s41467-019-08359-y.

(2) Yabuuchi, N.; Kubota, K.; Dahbi, M.; Komaba, S. Research Development on Sodium-Ion Batteries. *Chem. Rev.* **2014**, *114*, 11636-11682, DOI 10.1021/cr500192f.

(3) Hirsh, H. S.; Li, Y.; Tan, D. H. S.; Zhang, M.; Zhao, E.; Meng, Y. S. Sodium-Ion Batteries Paving the Way for Grid Energy Storage. *Adv. Energy Mater.* **2020**, *10*, 2001274, DOI 10.1002/aenm.202001274.

(4) Yang, C.; Xin, S.; Mai, L.; You, Y. Materials Design for High-Safety Sodium-Ion Battery. *Adv. Energy Mater.* **2021**, *11*, 2000974, DOI 10.1002/aenm.202000974.

(5) Shen, Z.; Guo, S.; Liu, C.; Sun, Y.; Chen, Z.; Tu, J.; Liu, S.; Cheng, J.; Xie, J.; Cao, G.; Zhao, X. Na-Rich Prussian White Cathodes for Long-Life Sodium-Ion Batteries. *ACS Sustain. Chem. Eng.* **2018**, *6*, 16121-16129, DOI 10.1021/acssuschemeng.8b02758.

(6) Kim, H.; Shakoor, R. A.; Park, C.; Lim, S. Y.; Kim, J.-S.; Jo, Y. N.; Cho, W.; Miyasaka, K.; Kahraman, R.; Jung, Y.; Choi, J. W. $Na_2FeP_2O_7$ as a Promising Iron-Based Pyrophosphate Cathode for Sodium Rechargeable Batteries: A Combined Experimental and Theoretical Study. *Adv. Funct. Mater.* **2013**, *23*, 1147-1155, DOI 10.1002/adfm.201201589.

(7) Bianchini, M.; Fauth, F.; Brisset, N.; Weill, F.; Suard, E.; Masquelier, C.; Croguennec, L. Comprehensive Investigation of the $Na_3V_2(PO_4)_2F_3$–$NaV_2(PO_4)_2F_3$ System by Operando High Resolution Synchrotron X-ray Diffraction. *Chem. Mater.* **2015**, *27*, 3009-3020, DOI 10.1021/acs.chemmater.5b00361.

(8) Zhang, B.; Ma, K.; Lv, X.; Shi, K.; Wang, Y.; Nian, Z.; Li, Y.; Wang, L.; Dai, L.; He, Z. Recent advances of NASICON-$Na_3V_2(PO_4)_3$ as cathode for sodium-ion batteries: Synthesis, modifications, and perspectives. *J. Alloys Compd.* **2021**, *867*, 159060, DOI 10.1016/j.jallcom.2021.159060.

(9) Jin, T.; Li, H.; Zhu, K.; Wang, P.-F.; Liu, P.; Jiao, L. Polyanion-type cathode materials for sodium-ion batteries. *Chem. Soc. Rev.* **2020**, *49*, 2342-2377, DOI 10.1039/C9CS00846B.

(10) Li, H.; Wang, T.; Wang, S.; Wang, X.; Xie, Y.; Hu, J.; Lai, Y.; Zhang, Z. Scalable Synthesis of the Na_2FePO_4F Cathode Through an Economical and Reliable Approach for Sodium-Ion Batteries. *ACS Sustain. Chem. Eng.* **2021**, *9*, 11798-11806, DOI 10.1021/acssuschemeng.1c03355.

(11) Cao, Y.; Liu, Y.; Zhao, D.; Xia, X.; Zhang, L.; Zhang, J.; Yang, H.; Xia, Y. Highly Stable $Na_3Fe_2(PO_4)_3$@Hard Carbon Sodium-Ion Full Cell for Low-Cost Energy Storage. *ACS Sustain. Chem. Eng.* **2020**, *8*, 1380-1387, DOI 10.1021/acssuschemeng.9b05098.

(12) Özdogru, B.; Dykes, H.; Gregory, D.; Saurel, D.; Murugesan, V.; Casas-Cabanas, M.; Çapraz, Ö. Ö. Elucidating cycling rate-dependent electrochemical strains in sodium iron phosphate cathodes for Na-ion batteries. *J. Power Sources* **2021**, *507*, 230297, DOI 10.1016/j.jpowsour.2021.23029.

(13) Rahmawati, F.; Faiz, Z.; Romadhona, D. A. N.; Saraswati, T. E.; Lestari, W. W. The performance of sodium ion battery with $NaFePO_4$ cathode prepared from local iron sand. *IOP Conf. Ser.: Mater. Sci. Eng.* **2020**, *902*, 012008, DOI 10.1088/1757-899x/902/1/012008.

(14) Xiao, J.; Li, X.; Tang, K.; Wang, D.; Long, M.; Gao, H.; Chen, W.; Liu, C.; Liu, H.; Wang, G. Recent progress of emerging cathode materials for sodium ion batteries. *Mater. Chem. Front.* **2021**, *5*, 3735-3764, DOI 10.1039/d1qm00179e.

(15) Moreau, P.; Guyomard, D.; Gaubicher, J.; Boucher, F. Structure and Stability of Sodium Intercalated Phases in Olivine $FePO_4$. *Chem. Mater.* **2010**, *22*, 4126-4128, DOI 10.1021/cm101377h.

(16) Sapra, S. K.; Pati, J.; Dwivedi, P. K.; Basu, S.; Chang, J. K.; Dhaka, R. S. A comprehensive review on recent advances of polyanionic cathode materials in Na - ion batteries for cost effective energy storage applications. *WIREs Energy Environ.* **2021**, *10*, e400, DOI 10.1002/wene.400.

(17) Hwang, J.; Matsumoto, K.; Orikasa, Y.; Katayama, M.; Inada, Y.; Nohira, T.; Hagiwara, R. Crystalline maricite $NaFePO_4$ as a positive electrode material for sodium secondary batteries operating at intermediate temperature. *J. Power Sources* **2018**, *377*, 80-86, DOI 10.1016/j.jpowsour.2017.12.003.

(18) Liu, Y.; Zhang, N.; Wang, F.; Liu, X.; Jiao, L.; Fan, L.-Z. Approaching the Downsizing Limit of Maricite $NaFePO_4$ toward High-Performance Cathode for Sodium-Ion Batteries. *Adv. Funct. Mater.* **2018**, *28*, 1801917, DOI 10.1002/adfm.201801917.

(19) Ong, S. P.; Chevrier, V. L.; Hautier, G.; Jain, A.; Moore, C.; Kim, S.; Ma, X.; Ceder, G. Voltage, stability and diffusion barrier differences between sodium-ion and lithium-ion intercalation materials. *Energy Environ. Sci.* **2011**, *4*, 3680-3688, DOI 10.1039/C1EE01782A.

(20) Zaghib, K.; Trottier, J.; Hovington, P.; Brochu, F.; Guerfi, A.; Mauger, A.; Julien, C. M. Characterization of Na-based phosphate as electrode materials for electrochemical cells. *J. Power Sources* **2011**, *196*, 9612-9617, DOI 10.1016/j.jpowsour.2011.06.061.

(21) Kim, J.; Seo, D.-H.; Kim, H.; Park, I.; Yoo, J.-K.; Jung, S.-K.; Park, Y.-U.; Goddard Iii, W. A.; Kang, K. Unexpected discovery of low-cost maricite $NaFePO_4$ as a high-performance electrode for Na-ion batteries. *Energy Environ. Sci.* **2015**, *8*, 540-545, DOI 10.1039/C4EE03215B.

(22) Hwang, J.; Matsumoto, K.; Nohira, T.; Hagiwara, R. Electrochemical Sodiation-desodiation of Maricite $NaFePO_4$ in Ionic Liquid Electrolyte. *Electrochemistry* **2017**, *85*, 675-679, DOI 10.5796/electrochemistry.85.675.

(23) Oh, S.-M.; Myung, S.-T.; Hassoun, J.; Scrosati, B.; Sun, Y.-K. Reversible $NaFePO_4$ electrode for sodium secondary batteries. *Electrochem. Commun.* **2012**, *22*, 149-152, DOI 10.1016/j.elecom.2012.06.014.

(24) Heubner, C.; Heiden, S.; Schneider, M.; Michaelis, A. In-situ preparation and electrochemical characterization of submicron sized $NaFePO_4$ cathode material for sodium-ion batteries. *Electrochim. Acta* **2017**, *233*, 78-84, DOI 10.1016/j.electacta.2017.02.107.

(25) Fang, Y.; Liu, Q.; Xiao, L.; Ai, X.; Yang, H.; Cao, Y. High-Performance Olivine $NaFePO_4$ Microsphere Cathode Synthesized by Aqueous Electrochemical Displacement Method for Sodium Ion Batteries. *ACS Appl. Mater. Interfaces* **2015**, *7*, 17977-17984, DOI 10.1021/acsami.5b04691.

(26) Wongittharom, N.; Lee, T.-C.; Wang, C.-H.; Wang, Y.-C.; Chang, J.-K. Electrochemical performance of $Na/NaFePO_4$ sodium-ion batteries with ionic liquid electrolytes. *J. Mater. Chem. A* **2014**, *2*, 5655-5661, DOI 10.1039/c3ta15273a.

(27) Casas-Cabanas, M.; Roddatis, V. V.; Saurel, D.; Kubiak, P.; Carretero-González, J.; Palomares, V.; Serras, P.; Rojo, T. Crystal chemistry of Na insertion/deinsertion in $FePO_4$–$NaFePO_4$. *J. Mater. Chem.* **2012**, *22*, 17421, DOI 10.1039/c2jm33639a.

(28) Fernández-Ropero, A. J.; Saurel, D.; Acebedo, B.; Rojo, T.; Casas-Cabanas, M. Electrochemical characterization of $NaFePO_4$ as positive electrode in aqueous sodium-ion batteries. *J. Power Sources* **2015**, *291*, 40-45, DOI 10.1016/j.jpowsour.2015.05.006.

(29) Berlanga, C.; Monterrubio, I.; Armand, M.; Rojo, T.; Galceran, M.; Casas-Cabanas, M. Cost-Effective Synthesis of Triphylite-$NaFePO_4$ Cathode: A Zero-Waste Process. *ACS Sustain. Chem. Eng.* **2019**, *8*, 725-730, DOI 10.1021/acssuschemeng.9b05736.

(30) Hsieh, H.-W.; Wang, C.-H.; Huang, A.-F.; Su, W.-N.; Hwang, B. J. Green chemical delithiation of lithium iron phosphate for energy storage application. *Chem. Eng. J.* **2021**, *418*, 129191, DOI 10.1016/j.cej.2021.129191.

(31) Gangaja, B.; Nair, S.; Santhanagopalan, D. Reuse, Recycle, and Regeneration of $LiFePO_4$ Cathode from Spent Lithium-Ion Batteries for Rechargeable Lithium- and Sodium-Ion Batteries. *ACS Sustain. Chem. Eng.* **2021**, *9*, 4711-4721, DOI 10.1021/acssuschemeng.0c08487.

(32) Mahandra, H.; Ghahreman, A. A sustainable process for selective recovery of lithium as lithium phosphate from spent $LiFePO_4$ batteries. *Resour. Conserv. Recycl.* **2021**, *175*, 105883, DOI 10.1016/j.resconrec.2021.105883.

(33) Hwang, J.; Takeuchi, K.; Matsumoto, K.; Hagiwara, R. NASICON vs. Na metal: a new counter electrode to evaluate electrodes for Na secondary batteries. *J. Mater. Chem. A* **2019**, *7*, 27057-27065, DOI 10.1039/c9ta09036c.

(34) Rodríguez-Carvajal, J. Recent advances in magnetic structure determination by neutron powder diffraction. *Phys. B: Condens. Matter* **1993**, *192*, 55-69, DOI 10.1016/0921-4526(93)90108-I.

(35) Gangadharan, R.; Namboodiri, P. N. N.; Prasad, K. V.; Viswanathan, R. The lithium—thionyl chloride battery — a review. *J. Power Sources* **1979**, *4*, 1-9, DOI 10.1016/0378-7753(79)80032-4.

(36) Venkatasetty, H. V.; Saathoff, D. J. Properties of $LiAlCl_4$ - $SOCl_2$ Solutions for Li / $SOCl_2$ Battery. *J. Electrochem. Soc.* **1981**, *128*, 773-777, DOI 10.1149/1.2127503.

(37) Grundish, N.; Amos, C.; Goodenough, J. B. Communication—Characterization of $LiAlCl_4 \cdot xSO_2$ Inorganic Liquid Li^+ Electrolyte. *J. Electrochem. Soc.* **2018**, *165*, A1694-A1696, DOI 10.1149/2.0291809jes.

(38) Gao, T.; Wang, B.; Wang, F.; Li, R.; Wang, L.; Wang, D. $LiAlCl_4 \cdot 3SO_2$: a promising inorganic electrolyte for stable Li metal anode at room and low temperature. *Ionics* **2019**, *25*, 4137-4147, DOI 10.1007/s11581-019-02994-7.

(39) Tanibata, N.; Takimoto, S.; Nakano, K.; Takeda, H.; Nakayama, M.; Sumi, H. Metastable Chloride Solid Electrolyte with High Formability for Rechargeable All-Solid-State Lithium Metal Batteries. *ACS Mater. Lett.* **2020**, *2*, 880-886, DOI 10.1021/acsmaterialslett.0c00127.

(40) Andersson, A. S.; Kalska, B.; Haggstrom, L.; Thomas, J. O. Lithium extraction/insertion in $LiFePO_4$: an X-ray diffraction and Mossbauer spectroscopy study. *Solid State Ionics.* **2000**, *130*, 41-52, DOI 10.1016/S0167-2738(00)00311-8.

(41) Zhu, Y.; Xu, Y.; Liu, Y.; Luo, C.; Wang, C. Comparison of electrochemical performances of olivine $NaFePO_4$ in sodium-ion batteries and olivine $LiFePO_4$ in lithium-ion batteries. *Nanoscale* **2013**, *5*, 780-787, DOI 10.1039/c2nr32758a.

(42) Galceran, M.; Saurel, D.; Acebedo, B.; Roddatis, V. V.; Martin, E.; Rojo, T.; Casas-Cabanas, M. The mechanism of $NaFePO_4$ (de)sodiation determined by in situ X-ray diffraction. *Phys. Chem. Chem. Phys.* **2014**, *16*, 8837-8842, DOI 10.1039/c4cp01089b.

(43) Lu, J.; Chung, S. C.; Nishimura, S.-i.; Yamada, A. Phase Diagram of Olivine Na_xFePO_4 ($0 < x < 1$). *Chem. Mater.* **2013**, *25*, 4557-4565, DOI 10.1021/cm402617b.

(44) Swanson, H. E.; Tatge, E. Aluminum (Cubic). In *Standard X-ray Diffraction Powder Patterns*, Vol. 1; National Bureau of Standards, 1953; pp 11-12.

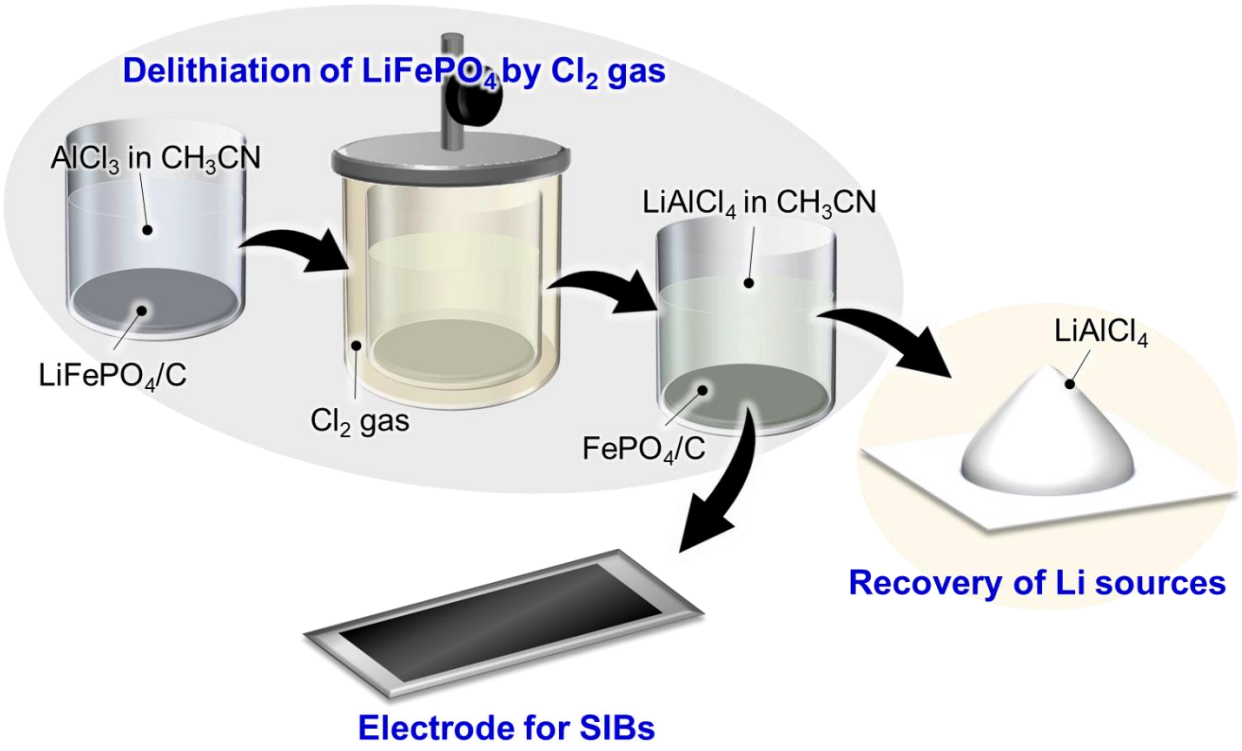

Figure 1. Schematic illustration of the synthetic route of $FePO_4/C$ by delithiation using Cl_2 gas and the recovery route of the Li sources.

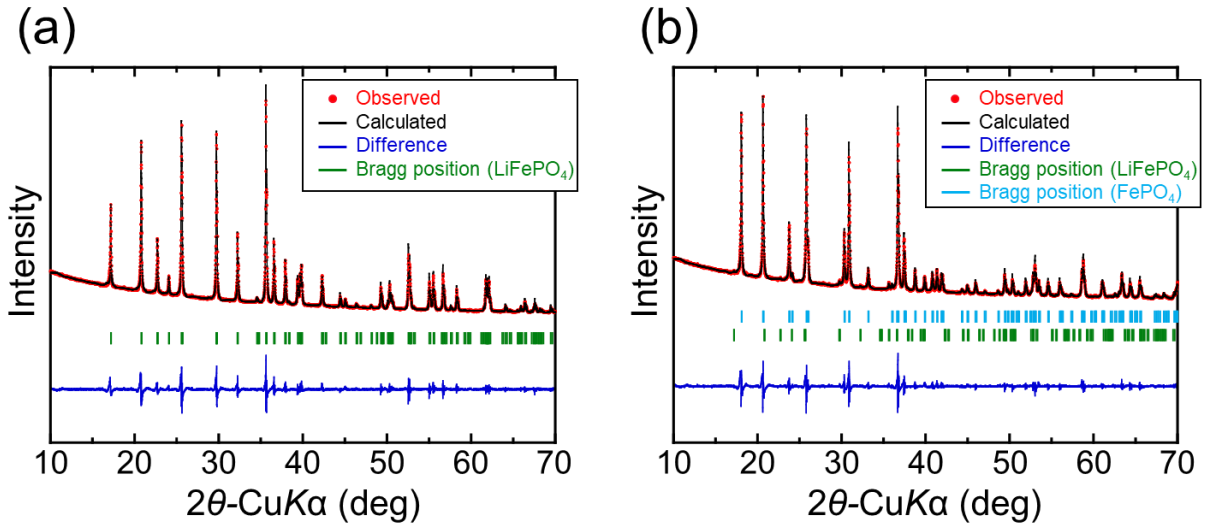

Figure 2. XRD patterns with Rietveld refinement results of (a) the pristine $LiFePO_4$/C and (b) the $FePO_4$/C obtained by delithiation of $LiFePO_4$/C using Cl_2 gas.

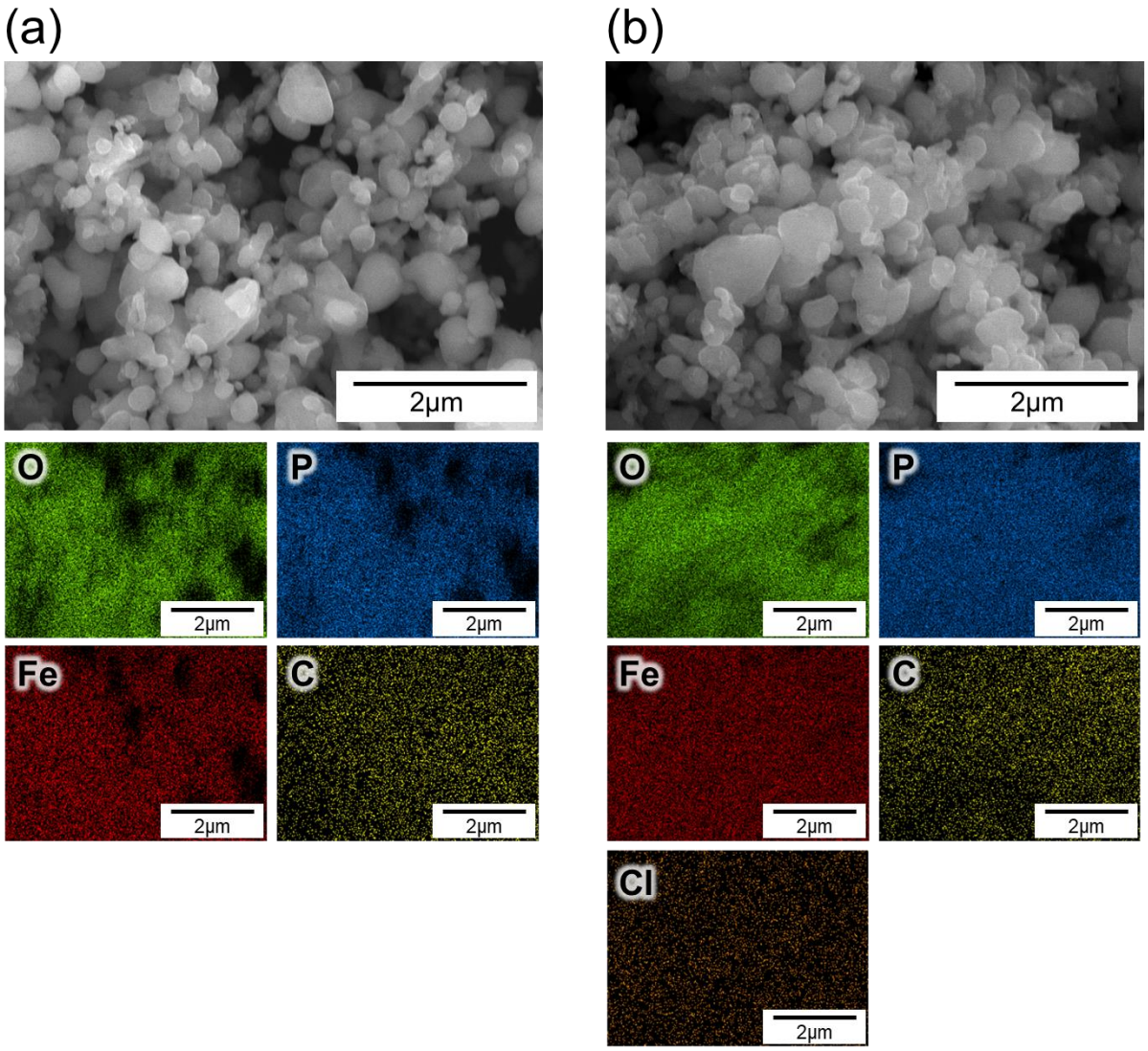

Figure 3. SEM images and EDX mappings of (a) the pristine $LiFePO_4/C$ and (b) the $FePO_4/C$ obtained by delithiation of $LiFePO_4/C$ using Cl_2 gas.

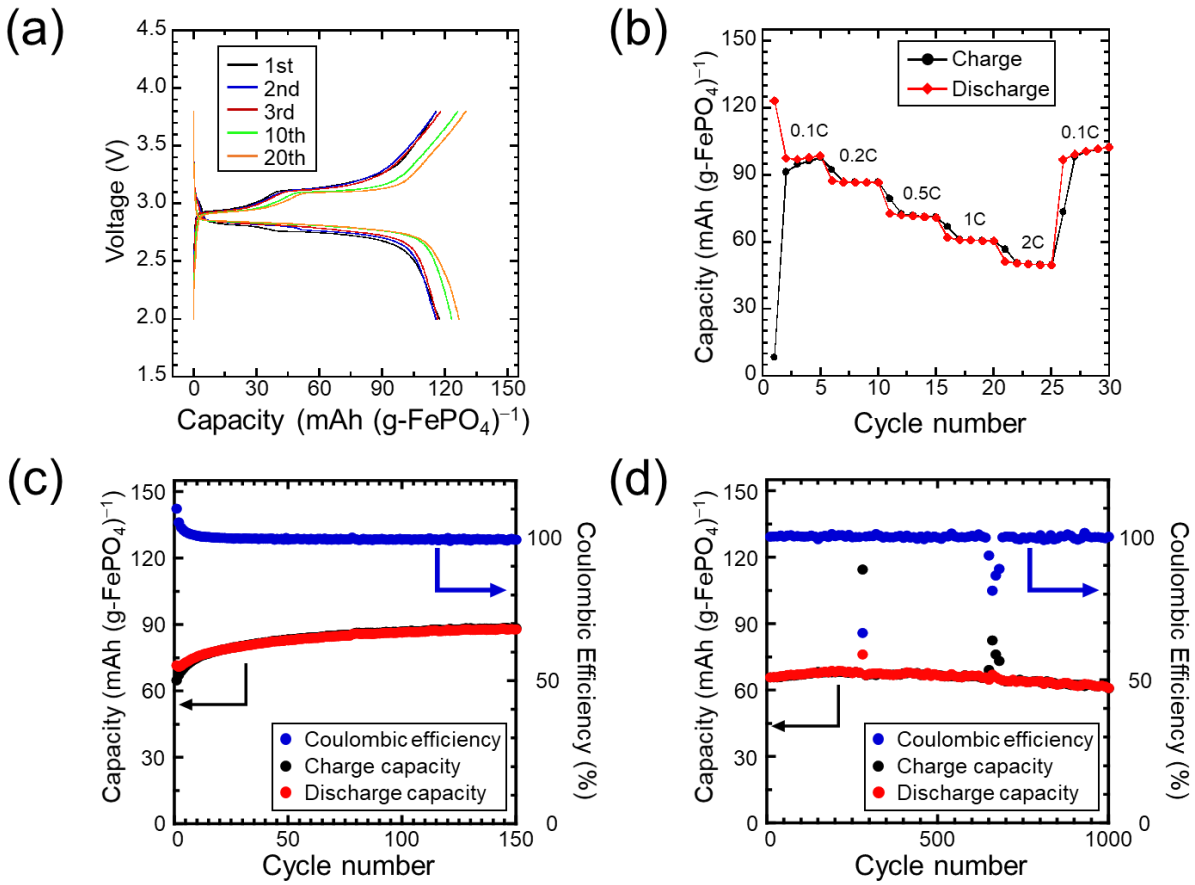

Figure 4. Electrochemical performance of the Na/$NaFePO_4$ cell with the 1 mol dm^{-3} $Na[PF_6]$-EC/DMC (1:1 v/v) with 3wt% of FEC addition. The $FePO_4$ obtained by chemical oxidation was preliminarily discharged at 0.05C prior to these tests. (a) Charge-discharge curves at 0.05C, (b) rate capability test, (c) cycle performance at 0.2C, and (d) cycle performance at 1C. Fluctuation observed during the cycle performance test over 1000 cycles is caused by physical shocks to the test cells.

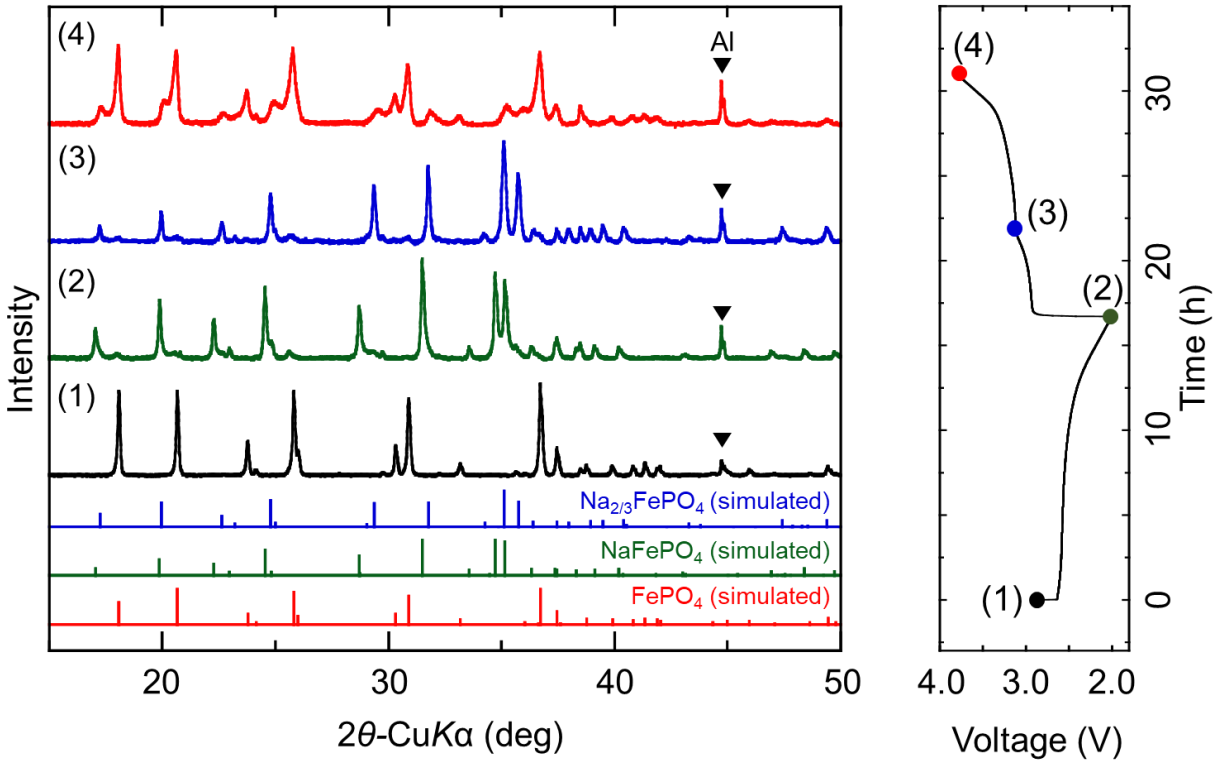

Figure 5. Ex-situ XRD patterns of the $FePO_4$/C electrodes at different states of charge. (1) Before preliminary discharge (pristine heterosite $FePO_4$), (2) after preliminary discharge (mainly assigned to $NaFePO_4$), (3) after charge to 32% SOC (mainly assigned to $Na_{2/3}FePO_4$), and (4) after full charge (mainly assigned to $FePO_4$). The simulated patterns are calculated based on crystallographic data in previous reports[15, 40] using VESTA software. The peak at 44.7° is assigned to Al metal.[44]

For Table of Contents Use Only

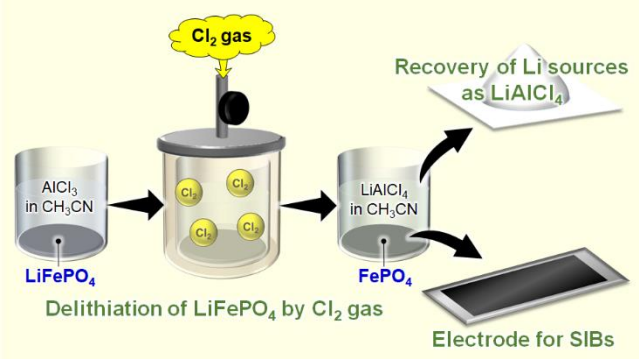

$FePO_4$ obtained by delithiation of $LiFePO_4$ with Cl_2 gas is used as an electrode for SIBs. The delithiated Li source can be recovered.